RESEARCH ARTICLE

A Correction Method Based on the Simulation and Experiment of Side Sled Collision

YI PANG[1,2,3]**, SHAW VOON WONG**[1,4]**, YONG HAN**[2]**, (Member, IEEE), AZIZAN AS'ARRY**[1]**, YAHAYA BIN AHMAD**[4]**, AND KEAN SHENG TAN**[5]

[1]Department of Mechanical and Manufacturing Engineering, Faculty of Engineering, Universiti Putra Malaysia (UPM), Serdang, Selangor 43400, Malaysia
[2]Fujian Province Key Laboratory of Advanced Design Manufacture for Bus, Xiamen University of Technology, Xiamen 361024, China
[3]Guangxi Shu Fang Technology Company Ltd., Liuzhou 545000, China
[4]Malaysian Institute of Road Safety Research, Kajang 43000, Malaysia
[5]National Defense University of Malaysia, Kuala Lumpur 57000, Malaysia

Corresponding author: Shaw Voon Wong (wongsv@upm.edu.my)

ABSTRACT In the context of conducting a side-impact collision test without side airbag for a specific vehicle model, an analysis of the injury value curve of the crash test dummy, when bench-marked against results from whole-vehicle testing, sled test and sled simulation, reveals two issues with the sled results: a delay in contact time and an excessively high peak value. This paper aims to analyze the problems arising from the simplification of the whole-vehicle model to the side-impact sled model. For the first time, these issues are addressed by correcting the sensor waveforms of the whole-vehicle test vehicle. Subsequently, by adjusting the input curves of the sled simulation model based on benchmarking the injury values of the side-impact sled dummy, a more accurate simulation of the dummy injury value curve is achieved compared to the experimental results. This approach represents an improvement in the substructure method for sled simulation, and its practicality and convenience have been validated through its application in a specific development vehicle project. The total score of the dummy injury in the experiment is 15.66, and the simulation is 15.76, the results are very close. The contact timing and peak value of chest, abdomen, and pelvis injury in the simulation are basically consistent with the experimental results. It offers a novel method for benchmarking dummy injuries, sled simulation, and sled testing in the context of side-impact collision condition, providing a new avenue for research and development in the automotive industry.

INDEX TERMS Vehicle side impact test, side sled test, side sled simulation, sensor waveform, dummy injury curve.

I. INTRODUCTION

In the early stages of automotive collision safety research, vehicle collision tests, including whole vehicle collision tests, sled tests, and component tests, are the primary methods employed [1], [2], [3]. In 1989, Tsinghua University in China established the first simplified whole vehicle collision test laboratory and conducted a series of collision test studies, achieving favorable results [4]. To reduce the cost of test development, restraint system manufacturers began using sled tests to develop airbags and seatbelt products. Compared to whole vehicle collision tests, this approach significantly reduced costs [5], [6], [7]. The research on sled test methods for side impact collisions began in the mid-1990s. Currently, there are well-established suppliers in the market for side impact sled test equipment, including Seattle Safety in the United States, IST in the United Kingdom, DSD in Austria, and Mitsubishi in Japan.

During side-impact collision tests, numerous factors affecting occupant safety are considered, including the vehicle's side structure intrusion velocity, intrusion depth, intrusion morphology, the stiffness of the door interior system, side

The associate editor coordinating the review of this manuscript and approving it for publication was P. Venkata Krishna.

restraint systems, and the occupant seat, among others. The side-impact sled test device is mainly composed of a crash pulse replicator, a door sled, and a seat sled [8].

Existing side-impact sled test devices from Seattle Safety and IST had some limitations, making it challenging to simulate whole vehicle collisions with low reliability. In response to these issues, Ha and Lee addressed the problem by modifying the structures of the door and seat in the sled test [9]. Miller et al. improved a compact sled system for linear impact, column impact, and side impact testing [10]. Aekbote et al. discovered a dynamic sled-to-sled testing method for simulating human responses in side-impact collisions [11]. Ma et al. proposed a dual-speed sled side-impact sled test method that was easy to implement in engineering. Mathematical simulations demonstrated a high correlation between injury values obtained from sled tests using the dual-speed sled curve and those obtained directly from door inner plate velocity curves [12]. Additionally, Gu et al. proposed an accelerated sled test method for side-impact column collisions based on multi-point intrusion [13].

The above various methods solved the problems that existed in their respective projects at that time. However, whether it was modifying the sled experimental equipment or modifying the input curve, the time and price costs were relatively high.

This study proposes an efficient correction method for conducting benchmarking work to solve the problem of contact time delay and high peak value of dummy injury curve. On one hand, it can save costs by not requiring alterations to the sled experimental equipment. On the other hand, it saves time by avoiding significant changes to the input curve of the experiment. By adjusting the input curves of door sensors through two steps "translation and reduction of peak values" the sled test and simulation input curves can be effectively corrected. The method has been applied to a project involving the development of side restraint systems for a specific vehicle model, resulting in significant improvements. This approach offers a highly efficient new method for sled testing and simulation, providing a useful contribution to the field.

II. METHODOLOGY

In the regulations governing the assessment of automotive collision safety performance, the rib deflection of the front dummy is scored as not exceeding 22 millimeters for 4 points, while exceeding this threshold resulted in a score of 0 points, The total score for the front dummy is 16 points [14]. As shown in Figure 1, this pertains to the side-impact MDB50 test. Sled testing, also known as carriage testing, is primarily utilized to substitute certain aspects of whole vehicle collision tests for the development of vehicle restraint systems. Due to the ability to conduct multiple tests on the same vehicle structure without the concern of damaging the overall vehicle structure during testing, couples with the short preparation time required for testing, sled

testing can effectively reduce the development cycle and cost of restraint systems [15], [16], [17], [18].
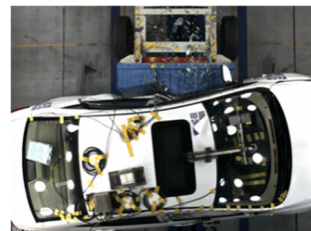

FIGURE 1. MDB50 test.

FIGURE 2. Door collides with dummy.

Sled testing is primarily employed to analyze the performance of vehicle components such as restraint systems, side trim stiffness, and seats. To obtain a reasonably simplified side-impact sled collision model, it is essential to understand the force transmission structure, paths, and factors influencing occupant safety in whole-vehicle side-impact collisions. The side-impact sled test aims to replicate the movement of the door inner panel on the sled, simulating the real vehicle's variable lateral displacement and the interaction process between the door and the dummy during collision tests [19].

Due to the uneven acceleration at various points on the door panel, current test devices can only simulate the movement of a specific point on the door inner panel. In practical applications, side-impact sled test devices are commonly used for side airbag development. On the other hand, chest injury criteria are of particular concern compared to other injury assessment metrics for side-impact dummies, as meeting the regulatory requirements for side impacts can be challenging. Consequently, the acceleration curve corresponding to the rib position of the dummy on the door inner panel is often chosen as the target curve for sled testing. This approach aims to address chest injury criteria while simultaneously considering injury response at other locations on the dummy [20].

The sled test for side-impact collisions serves as a cost-effective and time-efficient tool in the development of vehicle side restraint systems. Utilizing simulation methods allows for more rapid guidance in the design process, and the substructure method is a crucial means for optimizing the design of side-impact restraint systems [21]. Currently, there

FIGURE 3. Sled test model.

FIGURE 4. Sled simulation model.

are two main approaches to simulating the substructure of a simplified vehicle model in sled tests:

a. Extraction from whole vehicle side-impact simulation model: In this first method, the sub-structure simulation model is built based on the entire vehicle's side-impact simulation model. Information such as the deformation of the entire vehicle's door is extracted and used as input for the substructure simulation model.

b. Physical sled test-based sled simulation model: The second method involves building a sled simulation model based on actual physical sled tests. The key difference between these methods lies in the movement of the door and seat. However, aspects such as modeling the vehicle floor and positioning of the side-impact dummy remain consistent. Both of these methods play a crucial role in guiding the optimization design of side-impact restraint systems.

The second substructure method mentioned above typically involved using numerical values from sensor waveform curves on the door inner panel and corresponding dummy body parts as inputs for the simulation model. Comparative analyses are conducted on the calculation results of the whole vehicle model and substructure model after varying the structural parameters of the restraint system. The results indicates that the substructure model is suitable for optimizing the analysis of materials such as fillers, door trim panels, and door shapes [22].

This paper utilizes finite element simulation and experimentation to benchmark the results of the sled test against the whole vehicle test. The study focuses on comparing the injury value curves of the dummy between the sled
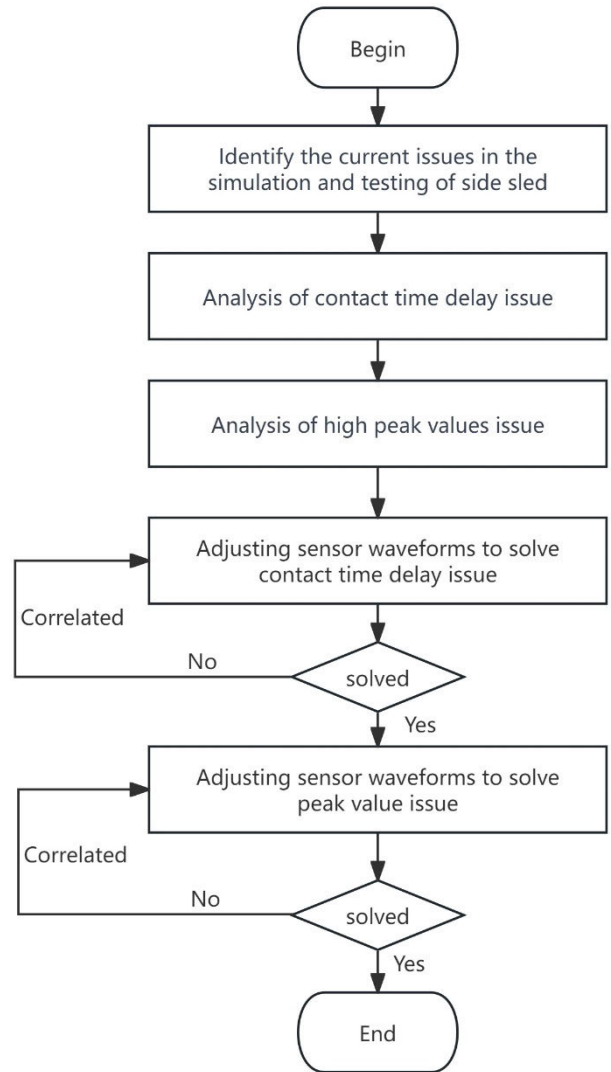

FIGURE 5. Flow chart of methodology.

test and the entire vehicle test. It identifies two issues, namely contact time delay and excessively large peak values. Through mathematical calculations and simulation solving, the paper determines the root causes of these problems. Subsequently, sensor velocity waveforms are adjusted to address these issues. Finally, the feasibility and efficiency of the proposed method are validated through simulation and experimental benchmarking results in engineering projects. The specific process is illustrated in Figure 5.

III. ISSUES ANALYSIS AND VERIFICATION OF SLED COLLISION
A. ISSUES ANALYSIS
When benchmarking the injury value curves of dummy on a sled simulation using the substructure method against a vehicle model without side airbags, two issues are identified:

1. Contact time delay: In comparing the injury value curves between the sled test and simulation, a delay in contact time

is observed. As depicted in Figure 6, during the whole vehicle MDB50 test, the door handle contacts the dummy's abdomen at 29 ms. However, in the sled simulation calculation at 30 ms, the door handle has not made contact with the dummy's abdomen, and there is still a distance of approximately 30 cm.
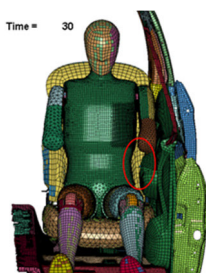

FIGURE 6. Vehicle test at 29ms.

FIGURE 7. Simulation at 30ms.

2. When benchmarking the injury value curves of a dummy between the sled test and simulation, the peak values are observed to be higher compared to the whole vehicle test. As shown in Figure 8, the injury value curve for the lower rib of the dummy indicates that the peak values in the sled test and sled simulation are higher than those in the whole vehicle test.
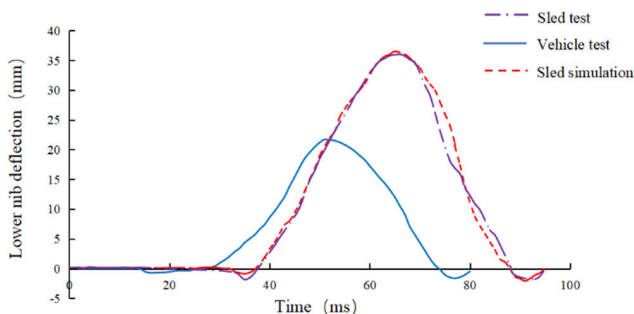

FIGURE 8. Deflection comparison of dummy's lower rib.

As shown in Figure 8, it depicts the deformation of the dummy's lower rib after colliding with the vehicle structure. In this context, the contact time for the whole vehicle collision occurs around 29 ms, while the contact time for the sled collision and simulation models is around 35 ms, indicating a delay of approximately 6 ms. The peak rib deformation in the whole vehicle test is approximately 22 mm, whereas

the deformation in the sled test and simulation is around 36 mm. Notably, both the peak deformations in the sled test and simulation are higher compared to the whole vehicle test.

B. VERIFICATION OF CONTACT TIME DELAY ISSUE

The analysis of the whole vehicle's side-impact test MDB50 involves solving a partial differential equation problem with unknown boundary conditions. This is a typical dynamic contact problem [23], [24], as illustrated in the simplified model shown in Figure 9. In the context of the whole vehicle side-impact collision, the collision motion between the movable barrier and the test vehicle follows the principle of energy conservation. The initial kinetic energy of the barrier vehicle is transformed into the deformation energy of the collision-avoidance vehicle and the car, as well as the internal energy related to friction between the floor and the vehicle, adhering to the energy conservation theorem [25].
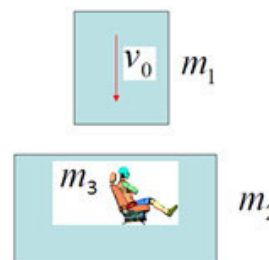

FIGURE 9. Side impact simplified diagram.

When the barrier vehicle collides with the test vehicle at an initial speed of 50 km/h, according to the law of energy conservation:

$$E_0 = \sum_{i=0}^{n} k_i + \sum_{i=0}^{n} u_i \tag{1}$$

$$E_0 = \frac{1}{2} m_1 v_0^2 \tag{2}$$

$$\frac{1}{2} m_1 v_0^2 = \frac{1}{2} m_1 v_1^2 + \frac{1}{2} m_2 v_2^2 + \frac{1}{2} m_3 v_3^2 + U_1 + U_2 + U_3 + U_{friction} \tag{3}$$

m_1 is the mass of the moving barrier vehicle, m_2 is the mass of the test vehicle, m_3 is the total mass of the dummy and seat, v_0 is the initial velocity of the moving barrier vehicle (50 km/h), v_1 is the velocity of moving barrier vehicle after collision, v_2 is the velocity of car after the collision, v_3 is the velocity of dummy after the collision, $_1$ is the deformation energy of the barrier vehicle's honeycomb aluminum, U_2 is the deformation energy of the car, $_3$ is the deformation energy of the dummy, $U_{friction}$ is the frictional energy between the floor and the barrier vehicle, and the floor and the car.

In the early stages of the whole vehicle collision, due to the inertia of the dummy and the lateral bending movement of the seat connected to the floor, the dummy undergoes lateral movement relative to the direction of the door before contacting the door trim. Figure 10 shows a video frame

FIGURE 10. The dummy moves towards the door.

35 ms after the start of the vehicle MDB50 test. At the midpoint of the seat, 35 ms after the barrier starts colliding with the test vehicle, it can be observed that the dummy has already experienced lateral movement relative to the door before contact. In contrast, in the sled collision test and sled simulation models, the dummy remains stationary before contacting the door trim because the seat and collision structure are disconnected, and there is no force transmitted from the seat structure to the dummy, as shown in Figure 11.
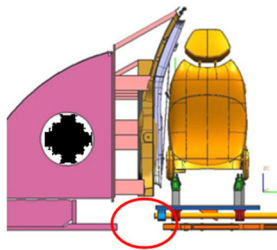

FIGURE 11. Seat structure schematic diagram of sled test.

Before the door collides with the dummy and seat as a whole, due to the inertia of the dummy and the lateral bending movement of the seat connected to the floor, the dummy undergoes lateral movement toward the direction of the door. Therefore, the actual velocity of the dummy relative to the door is corrected by adding the speed on the door sensor to the dummy's relative movement speed towards the door

$$v_{actual} = v_2 + v_3 \qquad (4)$$

v_{actual} is the actual speed between the car door and the dummy, v_2 is the sensor speed of the vehicle door inner panel, v_3 is the speed at which the dummy moves towards the car door. In the whole vehicle collision MDB50 test, the dummy's lateral movement relative to the door causes the actual collision velocity to be greater than the speed recorded by the door sensor. In contrast, in the sled test and sled simulation models, the dummy remains stationary before the door collides with it. There is no relative movement of the dummy towards the door. This discrepancy results in the sled test's dummy injury value curve waveform and the door contact time being delayed compared to the actual vehicle.

C. THE ISSUE OF HIGH INJURY VALUE

In the side-impact test of the deformable moving barrier vehicle (MDB50), the B-pillar and sill are two main force transmission paths. The force transmission through the B-pillar follows a vertical path, moving upward to transmit to the roof longitudinal beam and then laterally transferring through the roof support crossbeam. On the other hand, the sill serves as a longitudinal force transmission path, forwarding force to the A-pillar in the front and to the C-pillar in the rear [26], [27], [28].It also transmits laterally through the floor support beams, as illustrated in the diagram12 below.
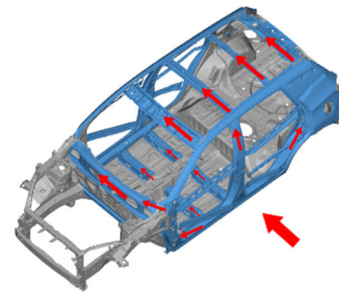

FIGURE 12. Force transmission path.

The side-impact sled test device primarily consists of a waveform reproducer, a door sled, and a seat sled, as shown in Figure 3, representing the sled test device for a particular vehicle model. Because the sled model lacks the sill structure, and in the energy distribution results of the side-impact MDB50 simulation for the entire vehicle, the sill beam and B-pillar absorbs about 20% of the energy in the entire system. Therefore, the sill beam and B-pillar are crucial structures in side-impact collisions [29], [30]. If the sensor waveform curves from the entire vehicle collision are used as input values for the sled simulation, neglecting the energy absorption by the sill, it may lead to an overestimation of the dummy injury values.

D. VERIFICATION OF HIGH INJURY VALUE

In both the whole vehicle collision test and the sled collision test, the forces acting on the door are variable and not directly measurable. However, in the whole vehicle collision (as shown in Figure 13) and the sled simulation model (as shown in Figure 7), the kinetic and internal energy of the door trim can be obtained from the corresponding simulation results, as illustrated in Figure 14 below.

Due to the similarity between the input velocity of the door in the simulation model and the acceleration sensor values in the actual vehicle, and the general consistency between the simplified model of the door and the actual vehicle model, the difference in kinetic energy of the door is not significant. However, the force transmission between the floor and seat affects the energy distribution in the entire vehicle system. As a result, the internal energy of the door trim is different between the whole vehicle model and the sled model.
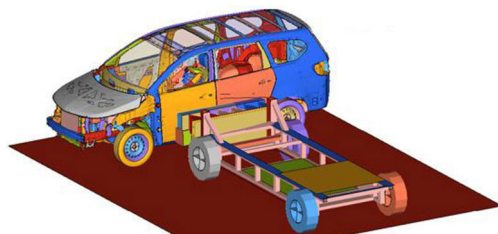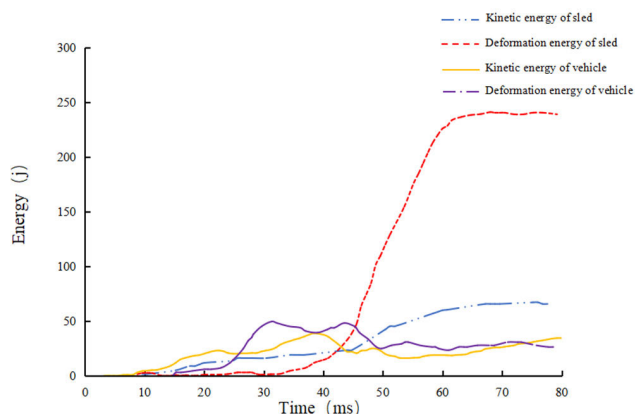
FIGURE 13. Vehicle MDB50 simulation model.

FIGURE 14. Comparison of door energy.

In the simulation model of the sled, the adoption of the "∗boundary-prescribed-motion" enforced loading method is causing a violation of the energy conservation principle [31]. Additionally, excessive deformation energy is observed in the interior of the car door. Comparing the internal energy of the door trim from Figure 14, it can be observed that the internal energy of the door trim in the sled model is 240.29J, while in the whole vehicle model, it is 66.75 J. The internal energy of the door trim in the sled model is approximately four times that of the whole vehicle model. In the experimental setup for the sled (shown as figure 11), the absence of force-absorbing structures such as threshold beams results in an excessive force impact on the crash test dummy directly by the car door. In short, these issues arise from simplifications made in the model and leads to an overestimation of the peak value in the dummy's chest injury value curve.

IV. CORRECT SENSOR WAVEFORM CURVE TO SOLVE ISSUES

Through the analysis and validation of the two issues mentioned above, to address these problems, this paper proposes a solution by modifying the waveform curve of the entire vehicle collision sensor to correct the sled simulation model. The waveform curve of the entire vehicle collision is generally obtained from the acceleration sensors attached to the door inner panel and B-pillar inner panel, where the red dots represent the sensor placement points. Rib1 represents the upper rib, Rib2 represents the middle rib, and Rib3

represents the lower rib, the locations of the arms, abdomen, pelvis, and tibia are shown in Figure 15.
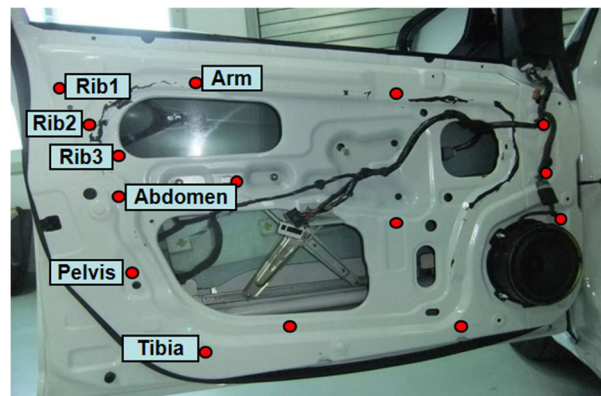

FIGURE 15. Vehicle side impact test sensor position.

The accelerometer sensor value corresponding to the position of the dummy's lower rib is taken, using CFC 60 to filter door acceleration and CFC 180 to filter lower rib injury curve with EVA test software. After filtering and integration processing, the sensor velocity curve of the door inner panel is obtained, as shown in Figure 16, the lower rib injury curve is obtained, as shown in Figure 19, the blue one.
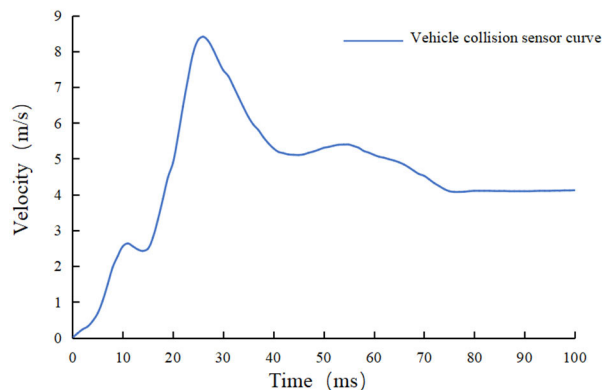

FIGURE 16. Door inner panel sensor speed curve.

A. MATHEMATICAL ANALYSIS OF CURVE CORRECTION
The velocity input curve for the sled simulation is shown in the above figure 17. Typically, the sensor curve at 100 ms is taken as the input backup. Although the finite element software Ls-dyna calculates up to 80 ms, and the curve beyond that is not invoked, it is convenient for later use after shifting. In the MDB50 side-impact test of the entire vehicle model, the dummy collides with the door at 30 ms. The timing of door contact for the sled test and sled simulation is delayed, and the displacement difference can be solved by shifting the sensor curve. In the first step, a 10 ms shift is applied to position a, where the velocity curves for the sled test and sled simulation start from 0. Position c, at 40 ms, represents the
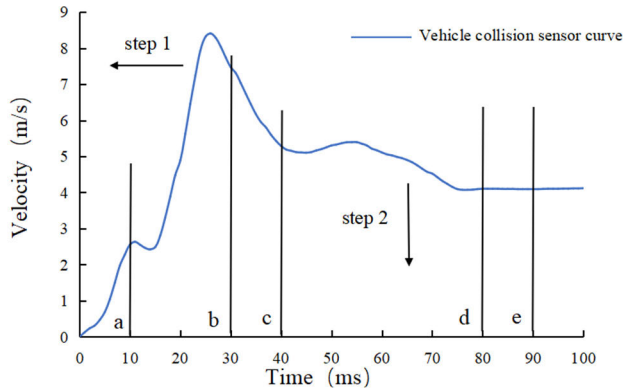
FIGURE 17. Speed curve correction diagram.

FIGURE 18. Contact time adjustment.

moment when the dummy collides with the door in the sled test and sled simulation.

$$S_a = \int_{t=0}^{t=a} vdt, \; S_b = \int_{t=0}^{t=b} vdt, \; S_c = \int_{t=0}^{t=c} vdt \qquad (5)$$

$$D = S_c - S_b = \int_{t=b}^{t=c} vdt - \int_{t=0}^{t=a} vdt \qquad (6)$$

The distance D between the door and the dummy can be obtained by integrating the velocity curve. The typical range for the shift value a is within 2-15 ms. For instance, If the dummy injury value curve experiences a contact time delay of 5 ms, then shifting a by 5 ms should be sufficient.

After translating the speed curve, the injury value of the dummy is too large. The second step is to reduce the contact force between door and dummy.

$$F = ma \qquad (7)$$

$$a = \frac{\partial v}{\partial t} \qquad (8)$$

The above formula indicates that to reduce the contact force F, it is sufficient to decrease the velocity of the car door. To reduce the velocity curve of the door, you can multiply the shifted curve in the c-e interval by a scaling factor. The specific scaling factor is determined based on the peak values of the injury value curves.

B. SLED SIMULATION AND BENCHMARKING VERIFICATION

For the corresponding correction of the whole vehicle collision test curve waveform, the first step is to adjust the contact time between the dummy and the door trim. According to the analysis of the contact time delay mentioned earlier, the contact time in the whole vehicle collision occurs around 29 ms, while for the sled collision and simulation models, the contact time is around 35 ms, with a delay of approximately 6 ms. To correct this, a shift of 6 ms (a value of 6) is applied, as shown in Figure 18.
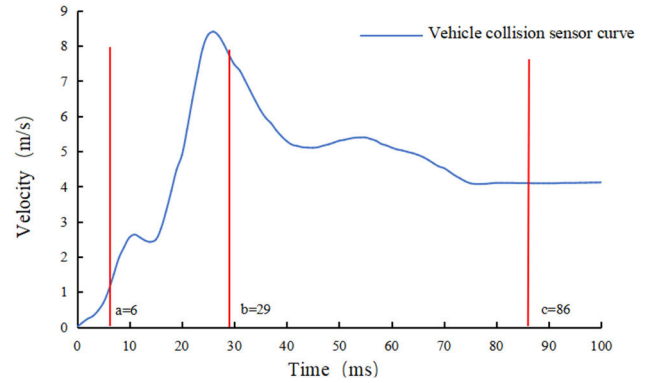
Utilize the pre-processing software Ansa to set up a sub-structure method simulation model. Employ the "∗boundary-prescribed-motion" keyword and conduct calculations using the finite element method software Ls-dyna. A curve representing the injury values of the dummy's lower ribs will be obtained from the result files. The injury value curve of the dummy's lower rib deflection obtained after adjusting the contact time is shown in Figure 19.
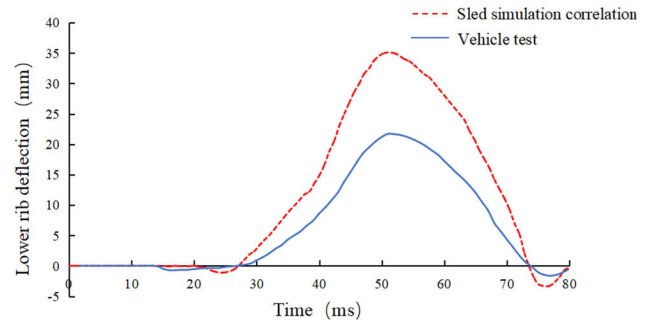

FIGURE 19. Deflection of lower rib after adjusting contact time.

Building upon the previous step, the next stage involves reducing the kinetic energy of the collision between the door and the dummy. The peak rib deformation value in the whole vehicle test is approximately 22 mm, while for the sled test and simulation, the deformation is around 36 mm. After dividing and taking the square root, a factor of 0.83 is obtained. Therefore, the velocity curve of the door sensor after 35 ms is multiplied by a factor of 0.83, as shown in Figure 20. This reduction in energy transferred to the dummy results in a corresponding decrease in the peak value of the dummy's injury curve. Finally, by fine-tuning the contact position corresponding to the injury location on the dummy with the door, the simulation model's injury value curve aligns with that of the whole vehicle collision test, completing the simulation benchmark analysis of dummy injury values. The obtained results are shown in Figure 21.

After correcting the waveform curves of the door inner panel sensors corresponding to other parts of the dummy
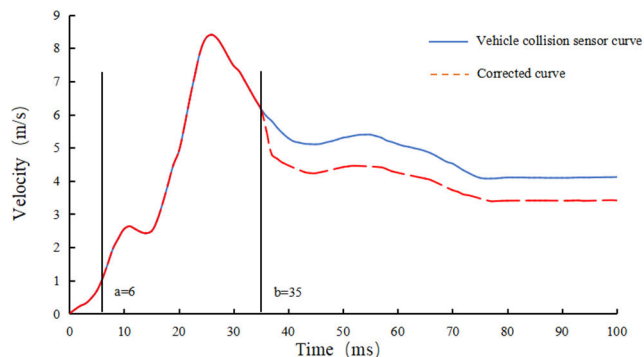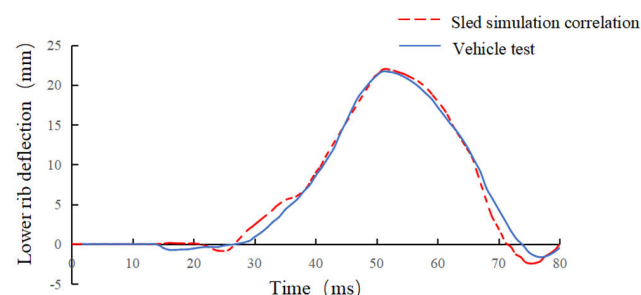
FIGURE 20. Injury value adjustment.

FIGURE 21. Deflection of lower ribs after adjusting peak value.

TABLE 1. Results comparison of dummy injury values.

Dummy	C-NCAP range	Vehicle test	Sled simulation
	3ms clip	44.8	57.3
Head	HIC36	98.1	114.5
	Upper rib V*C (m/s)	0.17	0.15
	Middle rib V*C (m/s)	0.16	0.16
Chest	Lower rib V*C (m/s)	0.16	0.19
	Upper rib deflection (mm)	18.9	19.0
	Middle rib deflection (mm)	19.0	21.0
	Lower rib deflection (mm)	21.7	22.0
Back place	Fy (KN)	0.28	0.22
T12	Fy (KN)	1.08	0.58
T12	Mx (N*m)	119.8	34.1
Abdomen	Fy (KN)	1.13	1.09
Pelvis	Fy (KN)	1.31	1.33
Conclusion	Driver scores	15.66	15.76

according to the above method, the injury value comparison as table 1 below is obtained.

V. CONCLUSION

This paper efficiently completes the simulation benchmarking of the dummy injury values in the side impact MDB50 test of a certain sedan by correcting the sensor input curves. The following conclusions are drawn:

(1) Analyzing the results of the whole vehicle test and the simulation on the sled, the force on the dummy's abdomen in the whole vehicle test is 1.13 kN, and in the sled simulation, it is 1.09 kN. For the pelvis force in test, the whole vehicle test result is 1.31 kN, and the simulation result is 1.33 kN. This indicates that the simulation model at the abdomen and pelvic regions is well benchmarked against the test model. The improved sub-structure method successfully addresses the significant differences in injury indicators at the abdomen and pelvic regions before model correction.

(2) Compared with previous modifications to the sled seat structure, which simulates the rotation and movement of the seat in whole vehicle collisions, the substructure method of modifying the sensor curve waveform in whole vehicle tests is more practical. It provides a balance between time and modification costs, as well as calculation accuracy. For injuries to the lower ribs of the chest, the MDB50 test is 22mm. Prior to implementing this method, the simulation calculation yields a result of 37mm, which deviates from the experimental result by 68.18%. However, after employing this method, the simulation calculation results in 21.7mm, with a deviation from the experimental results of only 1.36%. This method has led to a notable increase in the accuracy of the simulation calculation results by 66.82%. This conclusion is further validated by comparing the other results of dummy injury values in the simulation benchmarking against whole vehicle tests shown as the table 1.

(3) The simulation benchmarking and validation on the sled demonstrate that this method can be applied to sled tests. It provides a new approach for benchmarking and testing dummy injuries in side-impact sled simulations and tests for automobiles.

REFERENCES

[1] K. U. Schmitt, P. F. Niederer, M. H. Muser, and F. Walz, *Trauma Biomechanics: Accidental Injury in Traffic and Sports*, 2010, pp. 1–249.

[2] G. Naga Alekhya, C. B. N. S. Abhishikt, and B. Ramachandran, "A recent investigation on design aspects of vehicle crash analysis in India," *Mater. Today, Proc.*, vol. 33, pp. 4479–4485, Jul. 2020, doi: 10.1016/j.matpr.2020.07.713.

[3] E. A. Sribnick, J. A. Mansfield, C. Rhodes, V. Fullaway, and J. H. Bolte, "Biomechanical effects of a halo orthotic on a pediatric anthropomorphic test device in a simulated frontal motor vehicle collision," *Traffic Injury Prevention*, vol. 23, no. 8, pp. 500–503, Nov. 2022, doi: 10.1080/15389588.2022.2115837.

[4] L. Hu, X. Bao, M. Lin, C. Yu, and F. Wang, "Research on risky driving behavior evaluation model based on CIDAS real data," *Proc. Inst. Mech. Eng., D, J. Automobile Eng.*, vol. 235, no. 8, pp. 2176–2187, Jul. 2021, doi: 10.1177/0954407020985972.

[5] J. Zhang, X. Wang, and S. Huang, "Research on automobile air bag system," *Qinghua Daxue Xue bao/J. Tsinghua Univ.*, vol. 37, no. 11, pp. 69–72, 1997.

[6] C. S. Parenteau, D. C. Viano, and R. Burnett, "Second-row occupant responses with and without intrusion in rear sled and crash tests," *Traffic Injury Prevention*, vol. 22, no. 1, pp. 43–50, Jan. 2021, doi: 10.1080/15389588.2020.1842380.

[7] C. Ngiamngamsri and S. Chanthanumataporn, "Study on using waste tires to control crash pulse of sled test," *Mater. Today, Proc.*, vol. 77, pp. 1106–1111, Aug. 2023, doi: 10.1016/j.matpr.2022.11.396.

[8] P. M. Miller and H. Gu, "Sled testing procedure for side impact airbag development," in *Proc. SAE Tech. Paper Ser.*, Feb. 1997, doi: 10.4271/970570.

[9] Y.-H. Ha and B.-W. Lee, "A device and test methodology for side impact crash simulation using a frontal crash simulator and two hydraulic brake systems," in *Proc. SAE Tech. Paper Ser.*, Mar. 2000, doi: 10.4271/2000-01-0047.

[10] P. M. Miller, T. Nowak, and W. Macklem, "A compact sled system for linear impact, pole impact, and side impact testing," in *Proc. SAE Tech. Paper Ser.*, Mar. 2002, doi: 10.4271/2002-01-0695.

[11] K. Aekbote, J. Sobick, L. Zhao, J. E. Abramczyk, M. Maltarich, M. Stiyer, and T. Bailey, "A dynamic sled-to-sled test methodology for simulating dummy responses in side impact," in *Proc. SAE Tech. Paper Ser.*, Apr. 2007, doi: 10.4271/2007-01-0710.

[12] M. Zhixiong, "Research on vehicle sled test methodology and mathematical simulation technique of side restraint system," Ph.D. dissertation, School Automot. Eng., Wuhan Univ. Technol., Wuhan, China, 2008, doi: 10.7666/d.y1365777.

[13] H. Gu, P. Zhou, Y. He, and L. Lou, "Research on side pole impact test method of accelerating sled based on multi-point intrusion," in *Proc. Int. Conf. Mechatronics Eng. Artif. Intell. (MEAI)*, Mar. 2023.

[14] *C-NCAP Management Rules 2018 Edition*, China Automot. Technol. Res. Center, Tianjin, China, 2018.

[15] N. Yoganandan, H. Hauschild, J. Humm, Y. Purushothaman, and F. A. Pintar, "THOR dummy chest deflection response in oblique and lateral far-side sled tests," *Traffic Injury Prevention*, vol. 20, no. 1, pp. 32–37, Jun. 2019, doi: 10.1080/15389588.2019.1593389.

[16] S. Umale, H. Hauschild, J. Humm, K. Driesslein, and N. Yoganandan, "Effectiveness of center-mounted airbag in far-side impacts based on THOR sled tests," *Traffic Injury Prevention*, vol. 20, no. 7, pp. 726–731, Oct. 2019, doi: 10.1080/15389588.2019.1650266.

[17] Y. Purushothaman, J. Humm, D. Jebaseelan, and N. Yoganandan, "Compression-based injury variables from chestbands in far-side impact THOR sled tests," *Traffic Injury Prevention*, vol. 20, no. 2, pp. 179–182, Nov. 2019, doi: 10.1080/15389588.2019.1661681.

[18] H. W. Hauschild, J. R. Humm, F. A. Pintar, N. Yoganandan, B. Kaufman, J. Kim, M. R. Maltese, and K. B. Arbogast, "Protection of children in forward-facing child restraint systems during oblique side impact sled tests: Intrusion and tether effects," *Traffic Injury Prevention*, vol. 17, no. 1, pp. 156–162, Sep. 2016, doi: 10.1080/15389588.2016.1194982.

[19] T.-L. Teng, K.-C. Chang, C.-H. Wu, and J.-H. Lee, "Development and validation of side impact sled testing FE model," in *Proc. SAE Tech. Paper Ser.*, Apr. 2006, doi: 10.4271/2006-01-0248.

[20] N. Yoganandan and F. A. Pintar, "Responses of side impact dummies in sled tests," *Accident Anal. Prevention*, vol. 37, no. 3, pp. 495–503, May 2005, doi: 10.1016/j.aap.2004.12.007.

[21] N. Yoganandan, J. R. Humm, and F. A. Pintar, "Modular and scalable load-wall sled buck for pure-lateral and oblique side impact tests," *J. Biomech.*, vol. 45, no. 8, pp. 1546–1549, May 2012, doi: 10.1016/j.jbiomech.2012.03.002.

[22] C. A. Markusic and R. Songade, "Simplified side impact FE model—SSM," in *Proc. SAE Tech. Paper Ser.*, Apr. 2015, doi: 10.4271/2015-01-1486.

[23] D. Serfozo and B. Pere, "Application analysis of time stepping methods for impact problems," *Pollack Periodica*, vol. 17, no. 3, pp. 30–35, Sep. 2022, doi: 10.1556/606.2022.00599.

[24] X. Zhou, L. Jing, and X. Ma, "Dynamic finite element simulation of wheel-rail contact response for the curved track case," *Transport*, vol. 37, no. 5, pp. 357–372, Dec. 2022, doi: 10.3846/transport.2022.18292.

[25] R. B. Nallamothu and M. Y. Yihunie, "Design and analysis of sedan car B-pillar outer panel using Abirbara with S-glass fiber hybrid composites," in *Recent Trends in Mechanical Engineering* (Lecture Notes in Mechanical Engineering), vol. 26, 2021, pp. 419–432, doi: 10.1007/978-981-15-7557-0_37.

[26] Z. Hongxue, W. Sanxia, L. Xiao, P. Zhifei, and Z. Guosheng, "Optimization for side structure of vehicle based on FEA," *Proc. Comput. Sci.*, vol. 208, pp. 196–205, Jan. 2022, doi: 10.1016/j.procs.2022.10.029.

[27] Q. Li and J. Yang, "Study of vehicle front structure crashworthiness based on pole impact with different position," in *Proc. 5th Int. Conf. Measuring Technol. Mechatronics Autom.*, Jan. 2013, pp. 1031–1035, doi: 10.1109/ICMTMA.2013.255.

[28] C. Ma, J. Zhang, and S. Huang, "Structural improvement for vehicle side impact based on the design of experiment methodology," *Qiche Gongcheng/Automot. Eng.*, vol. 36, no. 2, pp. 195–198, 2014.

[29] L. Ying, "Optimization of crashworthiness for tailored hot forming B-pillar based on side impact," *J. Mech. Eng.*, vol. 53, no. 12, pp. 102–109, 2017, doi: 10.3901/jme.2017.12.102.

[30] A. Kasaei, N. A. Aziz, A. Delgoshaei, S. M. Tahir, and A. Rezanoori, "Optimum gas tank locating in van vehicle—Front and side crash analysis consideration for passenger safety," *Eng. Solid Mech.*, vol. 9, no. 2, pp. 177–220, 2021, doi: 10.5267/j.esm.2020.12.002.

[31] Y. Ren, Z. Yu, X. Hua, J. Amdahl, Z. Zhang, and Z. Chen, "Experimental and numerical investigation on the deformation behaviors of large diameter steel tubes under concentrated lateral impact loads," *Int. J. Impact Eng.*, vol. 180, Oct. 2023, Art. no. 104696, doi: 10.1016/j.ijimpeng.2023.104696.
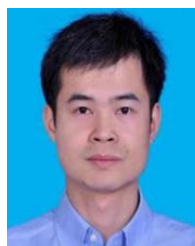
YI PANG received the B.S. and M.S. degrees in engineering mechanics from Hohai University, Nanjing, China, in 2006 and 2009, respectively. He is currently pursuing the Ph.D. degree in mechanical engineering with Universiti Putra Malaysia, Serdang, Malaysia.

He was an Associate Professor with Xiamen University of Technology, Xiamen, China. He also has prior experience as a Senior Engineer in automotive safety development with SGMW Automobile Plant and TAKATA's Technical Center. Later, he led a team of engineers in developing more than 20 vehicle models for various car manufacturers. His expertise and interests are centered around automotive crash safety and road traffic safety.

SHAW VOON WONG received the Ph.D. degree in mechanical engineering from Dublin City University, Ireland, in 2000.

He was the Former Director General of MIROS and the Founding Chairman of ASEAN NCAP. He is currently a Full Professor with the Department of Mechanical and Manufacturing Engineering and heading the Vehicle Engineering and Mobility Research Cluster, Universiti Putra Malaysia. He also holds the position of the Chairman of Malaysian Institute of Road Safety Research (MIROS) and the ASEAN Road Safety Centre. Furthermore, he chaired the International Working Group ISO TC 241 on good practices for implementing community safety management (ISO39002). Notably, he holds the position of the High-Level Panel Road Safety Expert of the Federation of International Automobile (FIA) and the UN Secretary-General's Special Envoy on Road Safety.

YONG HAN (Member, IEEE) received the Ph.D. degree in mechanical engineering from Hunan University, Changsha, China, in 2011. He was funded by China Scholarship Council to pursue a doctoral program with Nagoya University, Japan, from 2009 to 2011. He is currently a Professor with the School of Mechanical and Automotive Engineering, Xiamen University of Technology, Xiamen, China. His research interests include vehicle intelligence protection, VRUs (children, pedestrians, and two-wheelers) safety protection, and automobile active and passive safety integration, in-depth analysis of traffic accidents. He has registered 25 patents and published more than 110 papers in peer-reviewed international journals and conferences in his research areas.

YAHAYA BIN AHMAD received the M.S. degree in mechanical engineering from the King Mongkut's University of Technology North Bangkok, Thailand, in 2014. He is currently the Head of the Passenger Vehicle and Occupant Safety Unit and holds the position of the Technical Leader of ASEAN NCAP, within Malaysian Institute of Road Safety Research. In his role, he focuses on leading the assessment of vehicle safety, encompassing both passive and active safety technologies. Additionally, he takes charge of overseeing the implementation of Child Restraint System (CRS) Laws in Malaysia. Furthermore, he manages the crash test laboratory and test track at MIROS.

AZIZAN AS'ARRY was born in Kuala Lumpur, Malaysia. He received the bachelor's, master's, and Ph.D. degrees in mechanical engineering from Universiti Teknologi Malaysia, Malaysia, in 2007, 2009, and 2013, respectively. His major field of study is control and mechatronics. He is currently a Senior Lecturer with Universiti Putra Malaysia, Malaysia. His research interests include active force control, system identification, system modeling, and simulation.
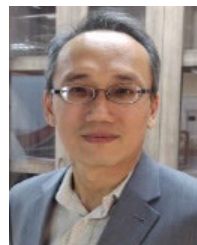
KEAN SHENG TAN received the Ph.D. degree in mechanical engineering from Universiti Putra Malaysia, in 2016. He is currently a Senior Lecturer with the Department of Mechanical Engineering, Faculty of Engineering, National Defense University of Malaysia. His research interests include finite element modeling, vehicle crash safety, and impact engineering of structural materials.

• • •